

Machine Learning for Shipwreck Segmentation from Side Scan Sonar Imagery: Dataset and Benchmark

Journal Title
XX(X):1–9
©The Author(s) 2024
Reprints and permission:
sagepub.co.uk/journalsPermissions.nav
DOI: 10.1177/ToBeAssigned
www.sagepub.com/

SAGE

Advait V. Sethuraman^{*,1}, Anja Sheppard^{*,1}, Onur Bagoren¹, Christopher Pinnow², Jamey Anderson², Timothy C. Havens², and Katherine A. Skinner¹

Abstract

Open-source benchmark datasets have been a critical component for advancing machine learning for robot perception in terrestrial applications. Benchmark datasets enable the widespread development of state-of-the-art machine learning methods, which require large datasets for training, validation, and thorough comparison to competing approaches. Underwater environments impose several operational challenges that hinder efforts to collect large benchmark datasets for marine robot perception. Furthermore, a low abundance of targets of interest relative to the size of the search space leads to increased time and cost required to collect useful datasets for a specific task. As a result, there is limited availability of labeled benchmark datasets for underwater applications. We present the AI4Shipwrecks dataset, which consists of 24 distinct shipwreck sites totaling 286 high-resolution labeled side scan sonar images to advance the state-of-the-art in autonomous sonar image understanding. We leverage the unique abundance of targets in Thunder Bay National Marine Sanctuary in Lake Huron, MI, to collect and compile a sonar imagery benchmark dataset through surveys with an autonomous underwater vehicle (AUV). We consulted with expert marine archaeologists for the labeling of robotically gathered data. We then leverage this dataset to perform benchmark experiments for comparison of state-of-the-art supervised segmentation methods, and we present insights on opportunities and open challenges for the field. The dataset and benchmarking tools will be released as an open-source benchmark dataset to spur innovation in machine learning for Great Lakes and ocean exploration. The dataset and accompanying software are available at <https://umfielddrobotics.github.io/ai4shipwrecks/>.

Keywords

Marine robotics, side scan sonar, deep learning, segmentation, benchmark datasets

1 Introduction

It is estimated that over 3 million undiscovered shipwrecks lie on the ocean floor Gonzalez et al. (2009). Locating these submerged archaeological sites enables research into important maritime assets of historical significance. However, searching over large areas and vast depths of the sea requires expensive and time-consuming surveys, which inhibits new discovery of shipwreck sites. Marine robotic platforms, including autonomous underwater vehicles (AUVs), have demonstrated potential to carry out efficient, cost-effective large-area surveys of marine environments returning hundreds of gigabytes worth of data. Still, the interpretation of sonar imagery to identify sites of interest requires manual expert review. This can take many months to complete, often requiring multiple surveys to verify potential new discoveries.

Automated processing of sonar data collected over large-area surveys has the potential to accelerate the discovery of new sites of interest. On land, machine learning has led to great advances in computer vision and robot perception tasks, including object detection, semantic segmentation, and scene understanding. State-of-the-art machine learning methods rely on labeled datasets for supervised training of neural networks to learn pixel-wise segmentation predictions. However, for underwater domains, there is limited availability of publicly available, labeled datasets for

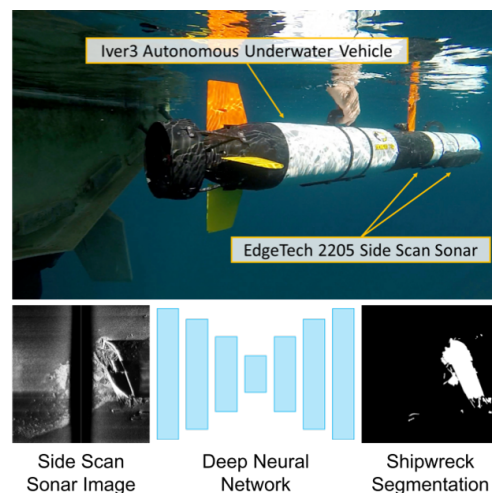


Figure 1. Our AI4Shipwrecks dataset aims to accelerate the development of shipwreck detection algorithms for sonar data collected onboard autonomous systems.

* denotes equal contribution

¹Department of Robotics, University of Michigan, Ann Arbor, MI, USA

²Great Lakes Research Center, Michigan Technological University, Houghton, MI, USA

Corresponding author:

Advait Sethuraman, 2505 Hayward St., Ann Arbor, MI 48109

Email: advaiths@umich.edu

arXiv:2401.14546v1 [cs.RO] 25 Jan 2024

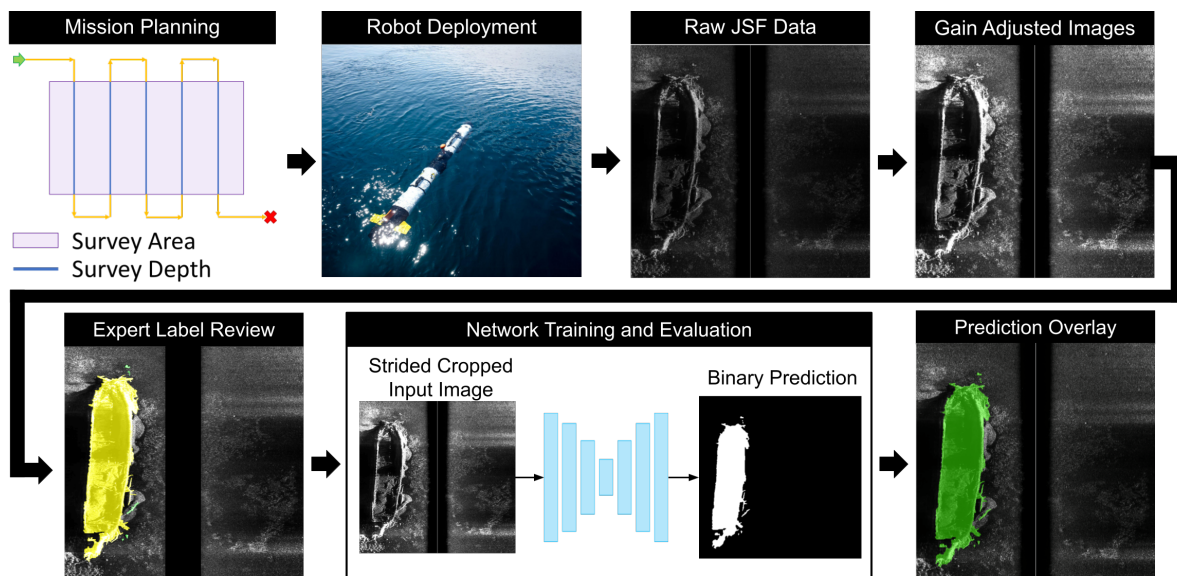


Figure 2. Data acquisition, processing, and network inference pipeline using the Iver3 autonomous underwater vehicle.

sonar data due to challenges, time, and expense associated with data collection Singh and Valdenegro-Toro (2021); Ochal et al (2020).

In this article we present a new dataset, AI4Shipwrecks, and we present benchmarking results for segmentation of shipwrecks from side scan sonar (SSS) imagery collected on an AUV (Fig. 1). This dataset was collected over the span of 5 weeks in Thunder Bay National Marine Sanctuary (TBNMS) in Lake Huron, Michigan, USA. Spanning 4,300-square-miles, TBNMS contains almost 100 known shipwreck sites and over 100 undiscovered sites. We leverage the unique abundance of known shipwreck sites to curate a rich dataset for investigating the application of machine learning for this task. In this paper, we present details of dataset collection and preparation for easy indexing of our dataset by machine learning pipelines. To encourage further advances in segmentation for side scan sonar, we report extensive results on our dataset from modern, state-of-the-art segmentation models. Lastly, we include discussion on lessons learned from our field expeditions and experiments to provide insight on future challenges and opportunities for machine learning for processing sonar data. The resulting dataset and benchmarking tools will be made publicly available as a benchmark dataset for segmentation from sonar imagery to enable future research in machine learning for ocean exploration.

2 Background

2.1 Object Segmentation in Sonar Imagery

Sonar is a popular perception sensor underwater due to its long operational range Lin et al. (2023). As a result, sonar image understanding algorithms are crucial for enabling autonomous underwater vehicles to operate in unstructured environments. Since many sonar images can be manipulated as single-channel images, sonar image understanding algorithms have a high overlap with object detection and segmentation algorithms from computer vision.

Recent work focuses on the application of data-driven deep neural networks for object detection and segmentation

in sonar imagery. The majority of work in object detection for sonar imagery involves retraining or fine-tuning existing object detection algorithms on task-specific datasets of sonar imagery Einsidler et al (2018); Yang et al. (2022). The unique nature of SSS imagery has also motivated the development of specialized network architectures Burguera and Bonin-Font (2020); Yang et al. (2022).

2.2 Datasets

Large, labeled, and publicly available SSS datasets incur high costs of collection and require expert analysis for labeling. As a result, there are very few options for evaluating the performance of object detection algorithms.

There has been recent interest in deep learning datasets for forward looking sonars (FLS) Singh and Valdenegro-Toro (2021); Choi et al. (2021); Xie et al. (2022); Santos et al. (2022). Singh and Valdenegro-Toro (2021) present an FLS dataset of debris in marine environments, but FLS is shorter range and has distinct sensor geometry compared to side scan sonar. Furthermore, the dataset is object-centric and captured in a controlled lab environment.

Although there is an abundance of unlabeled side scan datasets, they are also not immediately useful for benchmarking computer vision algorithms Bernardi et al. (2020). To the best of our knowledge, our AI4Shipwrecks dataset is the first publicly available, large, labeled dataset of side scan sonar images in the marine autonomy community.

2.3 Synthetic Datasets for Sonar

Simulation can produce low-cost, diverse, and labeled datasets for sonar image understanding Liu et al. (2021); Cerqueira et al. (2020); Sethuraman et al. (2023); Lee et al. (2018). Many simulators use ray-tracing techniques to render arbitrary 3D meshes Sethuraman et al. (2023); Cerqueira et al. (2020), while others use style-transfer techniques to mimic the noise and sensor models of sonars Lee et al. (2018); Sung et al. (2019). Although simulated data can help mitigate training data scarcity, it is still desirable to *evaluate* the performance of vision algorithms on a real test dataset. AI4Shipwrecks addresses this gap by leveraging the natural diversity of shipwreck sites in TBNMS. We present a

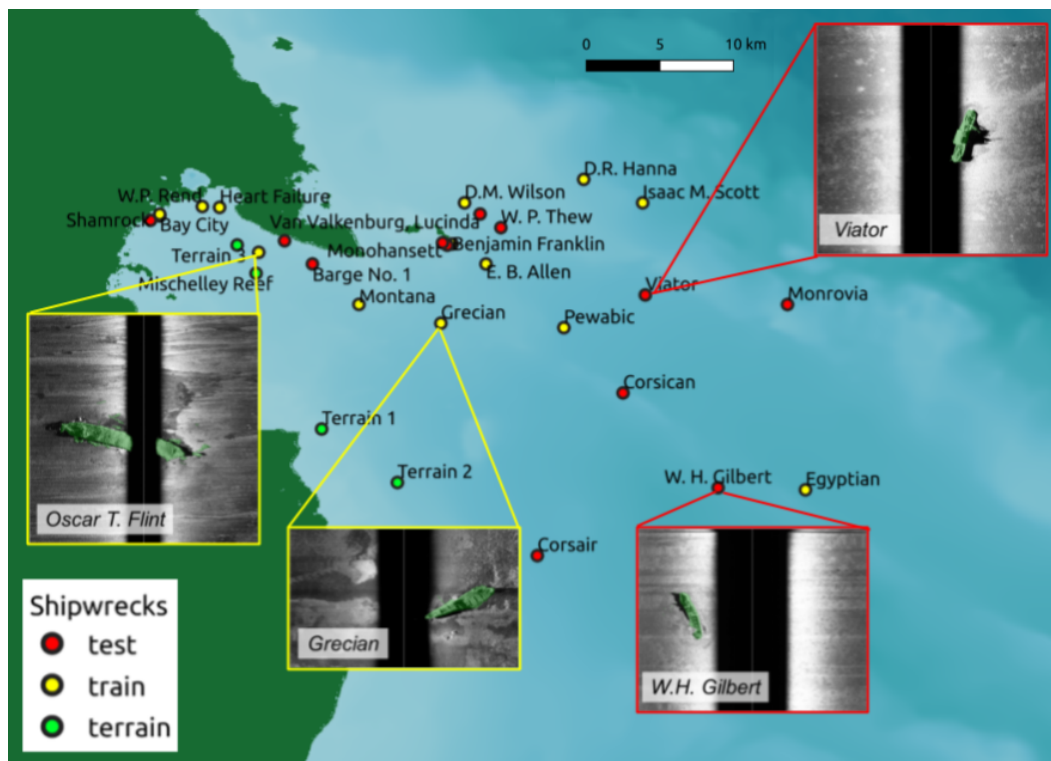


Figure 3. Map of survey sites in TBNMS. Callouts include example sonar data overlaid with ground truth labels. Color indicates sites that are included in testing (red) and training (yellow) splits, and locations of additional terrain surveys (green).

dataset representative of real shipwreck sites an AUV could encounter during autonomous surveys.

3 Technical Approach

Figure 2 provides an overview of the developed pipeline for acquiring sonar data for machine learning applications. First, data is collected through deploying an AUV for a large-area survey. The AUV carries out a pre-programmed survey mission to acquire sonar data. Once the data are returned, post-processing converts the raw sonar data format (.JSF) to standard image format (.PNG). The standard image format is further processed to be input into a deep neural network. The network outputs a prediction in the form of a binary per-pixel segmentation mask, which can be visualized as an overlay on the input sonar image.

3.1 Site Selection

Surveys were conducted in Thunder Bay National Marine Sanctuary (TBNMS) in Lake Huron, MI. Figure 3 shows shipwreck sites that were imaged in our surveys during four weeks over the course of two years. The abundance of known shipwreck targets in TBNMS was a crucial factor in our selection of this field site, as this enabled us to maximize the number of targets observed within a relatively constrained area and short timespan. These proposed survey regions were selected in coordination with scientists at TBNMS to cover a wide range of ship types, site relief, wreck characteristics, and water depth, prioritizing sites within a reasonable distance from the port of Alpena. This ensured that we could survey a maximum number of sites while still capturing variation across samples, providing a unique and valuable dataset for training machine learning methods. Furthermore, this large and diverse dataset allows

us to validate and thoroughly evaluate the accuracy and generalizability of developed methods.

3.2 Data Collection Platform

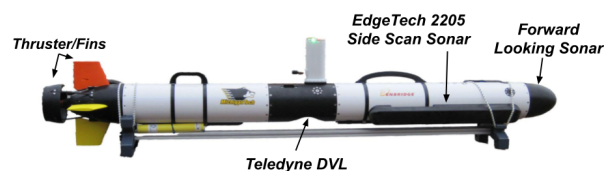


Figure 4. Iver3 data collection platform equipped with advanced localization and high-resolution seafloor mapping capabilities.

The surveys were conducted using the Michigan Technological University (MTU) Iver3 AUV (pictured in Fig. 4). Each survey mission was conducted by pre-programming a route to survey target sites. The AUV was programmed to capture SSS data while driving at a constant velocity of 2.5 knots, with a modular sensor payload that includes an EdgeTech 2205 dual frequency 600/1,600 kHz ultra-high resolution side scan sonar and 3D bathymetric system. The released imagery is produced from the low frequency sonar. An upgraded SBG Ellipse-A Inertial Measurement Unit (IMU) installed on the AUV's bathymetric sensor greatly improves the quality of this data, providing < 3 cm of resolution in both the horizontal and vertical planes. The AUV's Teledyne RDI Explorer Doppler Velocity Log (DVL) and high-accuracy compass provide absolute positional accuracy of 0.6 percent of the distance traveled underwater (CEP95). The AUV is also equipped with a forward-looking obstacle avoidance sonar. This combination of stability, highly accurate 3D autonomous

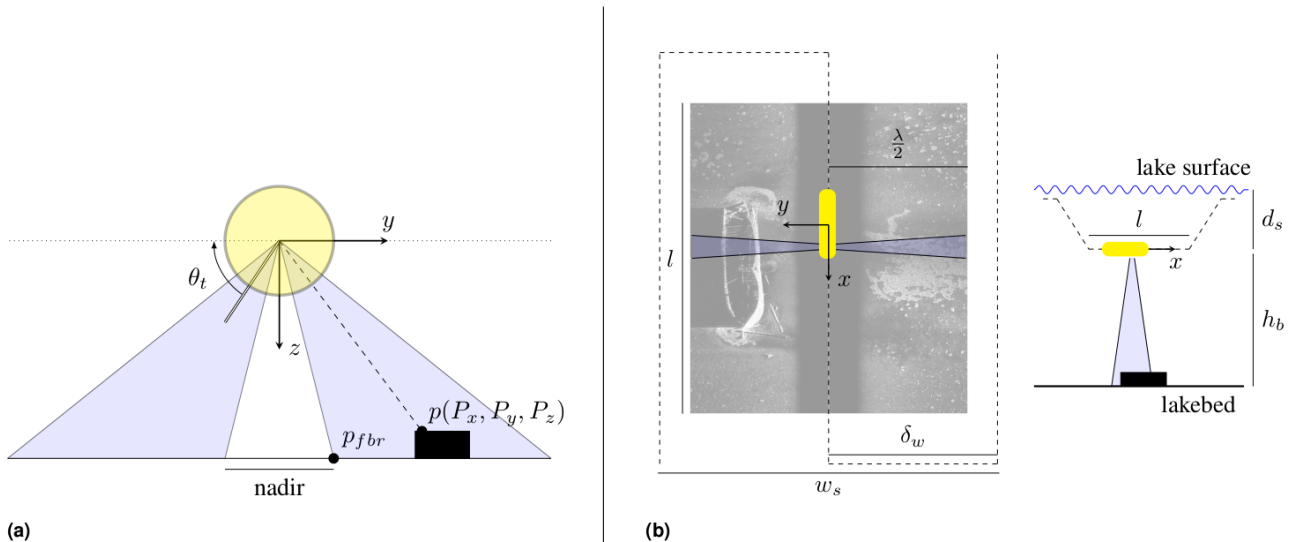


Figure 5. a) SSS sensor model detailing sensor tilt angle θ_t , first bottom return p_{fbr} , nadir gap, and ensonified point on object $p(P_x, P_y, P_z)$. The SSS field of view is shown in blue. b) The AUV (in yellow) performs a survey with half swath width $\frac{\lambda}{2}$, leg width δ_w , leg length l , and total survey width w_s . For each survey leg, the AUV dives to the depth from surface d_s or height from bottom h_b and resurfaces between legs to acquire a GPS lock.

positioning, obstacle avoidance, and ultra-high resolution sonar and camera makes the Iver3 platform optimal for this application.

3.3 Side Scan Sonar Sensor Model

A side scan sonar emits fan-shaped low and high-frequency acoustic pulses from two transducers aimed at the seabed floor. The signal travels through the water column and reflects off the terrain or other objects in the swath area before being received by the sensor. After a sonar chirp has been emitted, the sensor receives and bins the intensity of returns according to time-of-flight. On the horizontal axis, an SSS image is a histogram of return intensity at equally spaced intervals in time. Each histogram is accumulated in the vertical axis as the transducer moves to produce an image with two dimensions. The higher the echo signal intensity, the higher the pixel value in the resulting sonar image. Raw SSS imagery is single channel grayscale but can be viewed with various color palettes for improved visibility.

The sensor model is depicted in Fig. 5a and illustrates an acoustic beam that encounters an object at point $p(P_x, P_y, P_z)$. SSS typically has two identical transducer arrays mounted symmetrically on either side of the AUV at a fixed tilt angle θ_t . The first return from the sonar is called the first bottom return (p_{fbr}) and is used as an estimate of AUV altitude. There is typically a gap between the swath widths of both sides of the sensor resulting in a nadir gap with no coverage. This causes a black stripe down the center of a sonar image, as seen in Fig. 5b.

Although side scan sonar produces high resolution images of the environment, view-dependent shadowing effects, self-occlusion, material-dependent acoustic noise, and distortion make object detection a difficult task for both humans and automated algorithms. Figs. 6d-f illustrate common distortions and noise found in side scan sonar imagery.

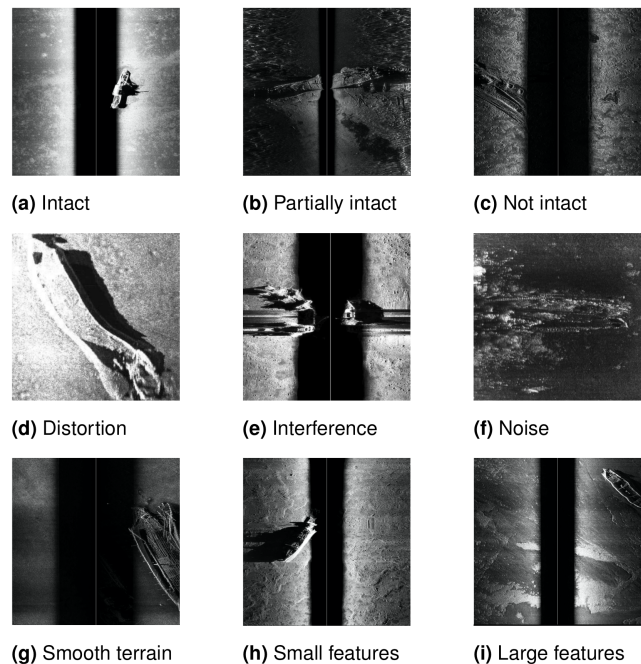


Figure 6. Images of wrecks highlighting levels of the three major categories used to split the dataset. Fig. 6a-6c represent the shipwreck conditions, Fig. 6d-6f represent different sonar quality conditions, and Fig. 6g-6i represent the terrain types.

3.4 AUV Survey Mission Planning

The Iver3 AUV has two standard patterns for pre-planned missions: lawnmower (LM) and object identification (OID). The LM pattern is a common down-and-back structure, as depicted by the dotted lines in Fig. 5b. In one leg of a LM survey, there are three stages: descent, survey, and ascent. The AUV must ascend, turn around, and then descend before collecting sonar data for each leg in order to geolocalize itself, as global positioning system (GPS) data is not available underwater. The leg length (l) in Fig. 5b denotes the distance that the AUV was underwater collecting SSS data, and the half-swath width ($\frac{\lambda}{2}$) describes the distance on

the seafloor covered by the fan-shaped sonar beams for one of the transducer arrays. w_s is the total survey width of a planned LM mission, and δ_w is the width of each individual leg. The AUV also takes in either a depth from surface (d_s) or a height from bottom (h_b) parameter which describes the altitude it will descend to before collecting SSS data.

3.5 Post-Processing

The Iver3 AUV stores each leg of a sonar survey separately as a .JSF file (proprietary format). These files are readable by the free Edgetech Discover software. The software allows for limited sonar image processing and exporting to .PNG. The Discover software normalizes the sonar image intensity and applies Time Varying Gain (TVG). As sound moves through water, absorption loss and spreading cause decreased signal strength. As a result, the returned echos from objects will also have reduced intensity. TVG addresses this shortcoming and ensures the intensity of the return on the sonar image is not range-dependent MacLennan (1986).

Pixel-wise labeling of the post-processed sonar images was conducted by a team of three researchers with shared labeling guidelines. The labels were then reviewed in-depth by a marine archaeologist from the State of Michigan who is an expert on the shipwrecks at TBNMS. There are two labels: “shipwreck” and “other.” “Shipwreck” consists of the primary wrecks as well as any debris. If part of the ship is obscured in an acoustic shadow, the label was extrapolated into the shadowed region to follow the expected shape of the wreck based off of expert knowledge. The labels are exported to a standard binary mask format where 0 represents the “other” class and 1 represents the “shipwreck” class.

As survey lengths (l) can vary for each mission, the resulting sonar images are of different lengths. The dataset provides full-sized images, but we square-cropped these images to be input to deep neural networks. Crops are generated by padding the full-size images from $h \times w$ to $H \times w$ according to

$$H = h + s - [(h - w)\%s] \quad (1)$$

where $s = 100$ is the stride length in pixels. Then, images of dimensions $w \times w$ are cropped every s pixels down the length of the padded image (H). A visualization of this process is shown in Fig. 7. The only other data processing step applied to the images is a normalization around 0 based on the mean and standard deviation of the pixel values of the entire dataset.

4 Dataset Organization

The dataset is organized by the SSS image and their corresponding labels. We provide the labels as segmentation masks of objects belonging to a shipwreck in the SSS image, including the shipwreck itself and any debris associated with the shipwreck. This includes parts of the shipwreck that may have come off from the shipwreck and parts of the ship that has been dislodged. The images and labels are separated into test and train sets using a 50/50 split. We select a 50/50 split to ensure that the test set is large enough to capture the variance of the shipwrecks sites, ensuring that the robustness of deep learning models can be evaluated through

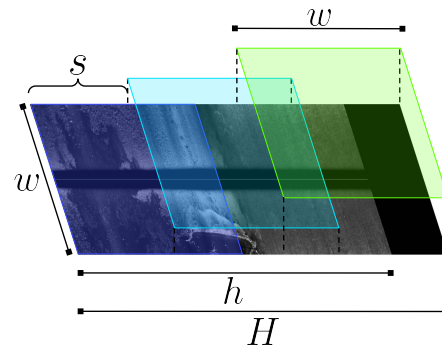


Figure 7. Visualization of the strided cropping of the original side scan sonar image to process before inputting into neural networks. Each colored square represents a $w \times w$ crop of the image, with a stride length of $s = 100$ px.

our dataset. In addition, the images are grouped on a per-site basis. This is done to ensure that SSS images that see the same terrain, shipwreck, or debris are not shared between the test and train sets of our dataset.

4.1 Released Dataset File Structure

In Fig. 8, the released data directory structure is shown. The data is split into test and train, according to our iterative approach as described in this paper. Within the test and train directories, the sonar images and their corresponding binary labels are stored. Each sonar image (.PNG format) corresponds to one leg of a survey mission. The site of the survey is indicated in the image file names.

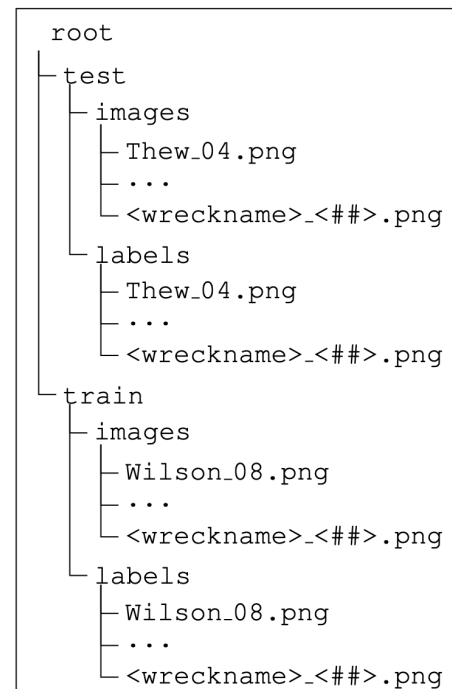


Figure 8. Directory structure of released dataset. Sonar images are sorted into test and train, and named according to their site.

4.2 Test-Train Split Selection

Our goal with the test-train split is to ensure that each set provides enough diversity of data for both the training

Table 1. Details of site characteristics, image quality, and number of images per site. Condition is in increasing order with 8 corresponding to most intact. SSS quality is in increasing order with 3 corresponding to highest quality. Terrain corresponds to categorical terrain types. *†,‡ denote shipwrecks that were imaged in a single survey and thus considered as a single “site.”

Name	Depth (m)	Length (m)	Beam (m)	Material	Condition	SSS Quality	Terrain	# Imgs.
Training								
<i>Alpena Steamer</i> †	–	–	–	–	4	2	C	10
<i>Bay City</i> †	3.4	44.5	8.8	Wood	4	2	C	10
<i>D.M. Wilson</i>	12.2	54.6	9.8	Wood	6	3	B	22
<i>D.R. Hanna</i>	41.1	162.2	17.1	Steel	8	2	A	5
<i>E.B. Allen</i>	30.5	40.8	7.9	Wood	6	3	D	24
<i>Egyptian</i>	79.2	70.7	11.0	Wood	5	2	D	15
<i>Grecian</i>	30.5	90.2	12.2	Steel	7	2	B	5
<i>Harvey Bissell</i> †	4.6	49.4	10.1	Wood	4	2	C	10
<i>Heart Failure</i>	5.5	–	–	Wood	2	1	B	12
<i>Isaac M. Scott</i>	53.3	159.7	16.5	Steel	8	2	C	6
<i>Montana</i>	19.2	71.9	11.0	Wood	6	3	A	8
<i>Oscar T. Flint</i>	9.1	66.4	11.3	Wood	5	2	A	22
<i>Pewabic</i>	50.3	61.0	9.4	Wood	6	2	A	5
<i>W.P. Rend</i>	5.2	87.5	12.2	Wood	5	3	A	11
Testing								
Artificial Reef	3.0	–	–	–	1	1	B	6
<i>Barge No. 1</i>	12.8	94.2	13.4	Wood	5	2	A	15
<i>B. Franklin</i> ‡	4.6	41.1	5.8	Wood	2	1	B	10
<i>Corsair</i>	55.5	40.8	7.3	Wood	5	2	C	4
<i>Corsican</i>	48.8	34.1	7.6	Wood	5	1	C	6
<i>James Davidson</i> ‡	10.7	30.5	9.1	Wood	4	1	A	10
<i>John F. Warner</i> *	2.7	38.4	7.9	Wood	3	1	B	6
<i>W.H. Gilbert</i>	77.7	100.0	12.8	Steel	8	3	C	6
<i>Haltiner Barge</i>	5.2	24.4	10.1	Wood	3	2	A	13
<i>L. Van Valkenburg</i>	18.3	39.0	7.9	Wood	5	3	B	19
<i>Monohansett</i> ‡	5.5	48.8	9.1	Wood	5	1	B	10
<i>Monrovia</i>	42.7	136.6	17.1	Steel	8	3	A	8
<i>Shamrock</i> *	3.4	44.5	9.1	Wood	2	1	B	6
<i>W.P. Thew</i>	25.6	40.2	7.3	Wood	5	3	A	17
<i>Viator</i>	57.3	70.7	10.1	Steel	8	2	C	11

and evaluation of deep learning models. We inform our split selection through both expert-informed and data-driven metrics, with the target of capturing the underlying distribution of the data as uniformly as possible. To inform the test-train split selection, we group the sites based on three major categories: shipwreck condition, sonar image quality (SIQ), and terrain type. For each site, a vector score of length three is assigned based on these quantitative and qualitative metrics. A 50/50 test-train split is then performed using an iterative stratification on our multi-labeled data Sechidis et al. (2011).

4.2.1 Wreck Condition: We leverage domain expert knowledge from scientists at TBNMS in order to assign wreck condition labels. Experts who have conducted dive surveys to inspect these ships provided a scale of 1-8 for wreck condition: 8 = complete and intact, 7 = complete but collapsed, 6 = semi-complete, 5 = partially intact, 4 = fragmented, 3 = fragmented and disarticulated, 2 = widely dispersed debris fields, and 1 = non-shipwreck cultural materials (e.g., artificial reef).

4.2.2 Sonar Image Quality Assessment: The sonar image quality (SIQ) assessment is done based on well-developed metrics for optical image quality assessment

(IQA). We utilize the no-reference, completely blind IQA metric Natural Image Quality Evaluator (NIQE) Mittal et al. (2013), which constructs a quality score from a natural scene statistic model trained on undistorted images. There are many challenges in evaluating the quality of a sonar image, the first of which being that many IQA metrics are targeted at measuring quality deterioration from compression. However, our sonar images are not compressed—rather, any distortion in the images is a result of when the Iver3 is surveying shallower sites, making it more vulnerable to drift from waves (Fig. 6d). If the shipwreck partially falls into the nadir, this can cause significant interference and acoustic shadows that disrupt the geometry of the wreck (Fig. 6e). Additionally, if the shipwreck falls into the outer edges of the sonar image, the increased noise of more distant acoustic returns causes significant noise in the final sonar image (Fig. 6f). Informed by the NIQE score, we assign classes of 1-3 to the images where 1 indicates poorer sonar image quality and 3 indicates higher image quality.

4.2.3 Terrain Type Assessment: We select the terrain type as a category for determining the test-train split, as the varying conditions of terrain can play a crucial role in the detection and segmentation of shipwrecks. This is most prominent in terrains that have a large amount of

texture, making it difficult even for humans to discern the shipwreck from the terrain, leading to either false negatives or false positives. We hence aim to have the terrains split evenly based on their characteristics observed from the SSS imagery. In order to determine the most even split across the data based on terrain, we utilize clustering methods.

Specifically, the clustering is done on the N-dimensional latent space of a Variational Auto Encoder (VAE) pre-trained on a large color image (RGB) dataset. The input images are pre-processed by applying white balancing. This is done in order to prevent the clustering based on image intensity; otherwise, the intensity differences across the dataset are too prominent. We use k -means clustering, yielding a partitioning on an image-to-image basis. Each image is grouped based on the site it belongs to, which is then used to inform the test-train split. We assign sites a class of A for terrains with small-scale texture, a class of B for terrains with large-scale texture, a class of C for smooth terrain, and a class of D for patchy terrain texture.

4.3 Dataset Statistics

The dataset consists of 286 images exported from the Discover software as high-resolution images. Note that despite the number of images being low, the average dimension of the images is $3,480 \times 1,728$ pixels. The width of each exported image is fixed at 1,728 pixels. The height varies across the 286 images due to it being dependent on the leg length of each survey. We note that by applying the strided-cropping, as described in Section 3.5, we can obtain 4,672 images of shape $1,728 \times 1,728$ pixels. Table 1 provides further details of each site, including material, ship length and ship beam (width) obtained from Thunder Bay National Marine Sanctuary (Accessed online: 2024), as well as classification details according to our data categorization for terrain type, sonar image quality, and wreck condition.

5 Experiments & Results

5.1 Baseline Comparison

We perform benchmark evaluations on a series of deep learning-based segmentation methods to evaluate the ability of state-of-the-art deep learning methods to segment shipwrecks from SSS imagery. Benchmark methods are selected to reflect the variety of deep learning-based segmentation models used in the vision community: Yang et al. (2022), ViT Adapter Chen et al. (2023), DeepLabV3 Chen et al. (2017), HRNet Wang et al. (2020), UNet Ronneberger et al. (2015), and Salient Object Detection (SOD) InSPyReNet Kim et al. (2022). The model with the longest training time was SOD, which took 14 hours on a single NVIDIA A100 GPU with 80Gb of memory. All baselines were trained on 512×512 images.

Each model is evaluated on an aggregate level with mean Intersection Over Union (mIoU), IoU for the “shipwreck” class (IoU_{ship}), IoU for the “other” class ($\text{IoU}_{\text{other}}$), F1 score, True Positive Rate (TPR), True Negative Rate (TNR), False Positive Rate (FPR), and False Negative Rate (FNR). Table 2 provides results across baselines, averaged across each site. Table 3 shows mIoU per site for each baseline. Segmentation predictions for all six baselines on three example sites are

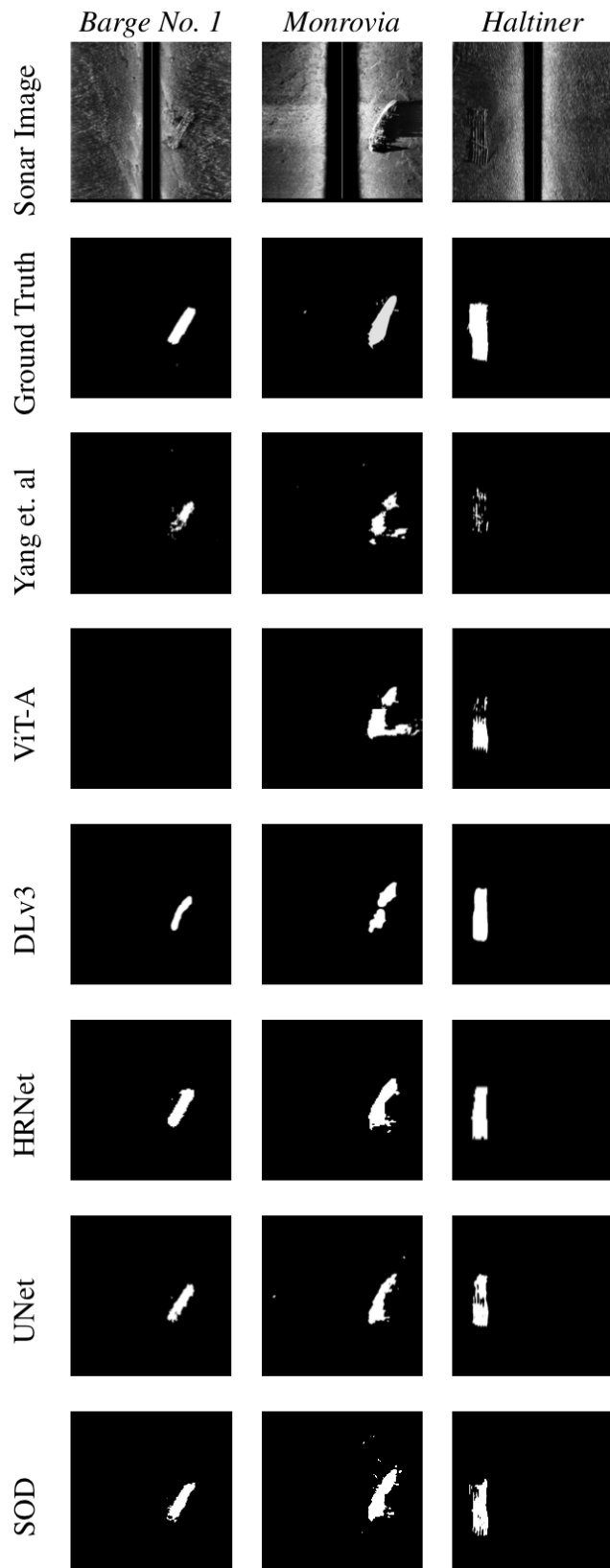


Figure 9. Shipwreck segmentation predictions from the baselines on *Barge No. 1*, *Monrovia*, and *Haltiner*

shown in Fig. 9. Across this comparison, the SOD model consistently outperformed or performed comparably against all other networks for the aggregate metrics. We performed all subsequent experiments with the SOD model.

Table 2. Aggregate baseline performance averaged across sites: metrics are computed per site and then the average is taken across all test sites for each metric. Metrics include mIoU, per-class IoU metrics, F1 Score, TPR, TNR, FPR, and FNR. \uparrow indicates higher is better. \downarrow indicates lower is better.

Baseline	mIoU \uparrow	IoU _{ship} \uparrow	IoU _{other} \uparrow	F1 Score \uparrow	TPR \uparrow	TNR \uparrow	FPR \downarrow	FNR \downarrow
Yang et. al	0.609	0.229	0.990	0.333	0.319	0.996	0.004	0.681
ViT-Adapter	0.637	0.283	0.991	0.395	0.488	0.995	0.005	0.512
DeepLabv3	0.678	0.363	0.992	0.473	0.485	0.996	0.004	0.515
HRNet	0.683	0.372	0.994	0.490	0.516	0.998	0.002	0.484
UNet	0.702	0.411	0.994	0.526	0.592	0.997	0.003	0.408
SOD	0.720	0.445	0.994	0.594	0.652	0.997	0.003	0.348

Table 3. Per-site mIoU compared across each baseline for each site. Higher is better (\uparrow).

	Artificial Reef	Barge No. 1	Corsair	Corsican	Davidson	W.H. Gilbert	Halter Barge	L. Van Valkenburg	Monohansett	Monrovia	Shamrock	W.P. Thew	Victor
Yang et. al	0.496	0.735	0.616	0.527	0.492	0.635	0.515	0.668	0.499	0.730	0.548	0.566	0.778
ViT-Adapter	0.498	0.704	0.771	0.541	0.499	0.501	0.680	0.564	0.736	0.724	0.673	0.576	0.812
DeepLabv3	0.495	0.834	0.765	0.518	0.514	0.828	0.730	0.814	0.515	0.693	0.572	0.700	0.831
HRNet	0.503	0.851	0.646	0.586	0.533	0.819	0.724	0.813	0.602	0.775	0.498	0.710	0.820
UNet	0.499	0.867	0.781	0.555	0.536	0.862	0.621	0.813	0.518	0.779	0.712	0.765	0.821
SOD	0.507	0.887	0.791	0.532	0.518	0.874	0.721	0.850	0.732	0.779	0.497	0.783	0.886

5.2 Train Set Size Experiment

Intuitively, a larger training set should lead to better learning conditions for the network and ultimately result in a more accurate model. We conducted an experiment where we gradually increased the size of the train set back up to the full set in order to observe the relationship between train set size and model performance for our dataset. As we increase the train set size, we evaluate model performance on a frozen test set. As shown in Fig. 10, we observe that test performance increases with increased training dataset size and the network performance plateaus at around six sites in the train set.

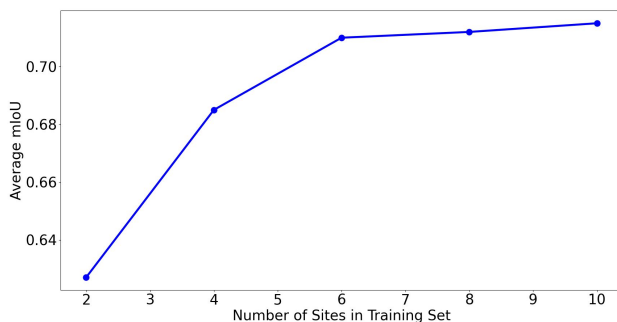


Figure 10. Results of the train set size experiment. Note the plateau in performance after six training sites.

6 Conclusion & Future Work

This work contributes AI4Shipwrecks, an open-source dataset for comparison of state-of-the-art deep neural networks for shipwreck segmentation from sonar imagery. While recent advances in deep learning have revolutionized the field of computer vision for terrestrial robotics, adoption of similar methods across marine applications is limited due to a lack of widely available data for development and direct comparison of results. We establish a benchmark for semantic segmentation of shipwrecks in the AI4Shipwrecks

dataset, and we provide comparison of current state-of-the-art deep neural networks for segmentation. The dataset and code for evaluation will be open-source to enable future research in machine learning for ocean exploration.

A promising direction for future work includes leveraging synthetic data to augment real sonar datasets for learning-based detection and segmentation tasks Lee et al. (2018); Sethuraman et al. (2022). Additionally, work should also focus on advancing network architecture to enable DNNs to learn from limited training data. Of notable interest, recent work has demonstrated the potential for few shot learning for object detection from marine optical and sonar imagery Ochal et al (2020). Few shot and one shot learning aim to effectively learn to represent a class of objects after seeing a few or single instance of that class, which is ideal for datasets with relatively low abundance of samples per class.

Acknowledgements

We would like to acknowledge the lives that were lost in shipwrecks throughout Thunder Bay National Marine Sanctuary. We would also like to thank the sanctuary scientists at Thunder Bay National Marine Sanctuary for supporting field experiments and labeling efforts.

Declaration of conflicting interests

The Authors declare that there is no conflict of interest.

Funding

The authors disclosed receipt of the following financial support for the research, authorship, and/or publication of this article: This work is supported by the NOAA Ocean Exploration program under Award #NA21OAR0110196.

References

Bernardi, M., Hosking, B., Petrioli, C., Bett, B.J., Jones, D., Huvenne, V.A., Marlow, R., Furlong, M., McPhail, S., and

- Munafo, A. (2020). Aurora a multi sensor dataset for robotic ocean exploration. DOI: 10.21227/nnms-te61. URL <https://dx.doi.org/10.21227/nnms-te61>.
- Burguera, A., and Bonin-Font, F. (2020). On-line multi-class segmentation of side-scan sonar imagery using an autonomous underwater vehicle. *Journal of Marine Science and Engineering*, 8(8): 557. DOI: 10.3390/jmse8080557.
- Cerqueira, R., Trocoli, T., Albiez, J., and Oliveira, L. (2020). A rasterized ray-tracer pipeline for real-time multi-device sonar simulation. *Graphical Models*, 111: 101086. DOI: <https://doi.org/10.1016/j.gmod.2020.101086>. URL <https://www.sciencedirect.com/science/article/pii/S1524070320300278>.
- Chen, L.C., Papandreou, G., Schroff, F., and Adam, H. (2017). Rethinking Atrous Convolution for Semantic Image Segmentation. *ArXiv:1706.05587* [cs].
- Chen, Z., Duan, Y., Wang, W., He, J., Lu, T., Dai, J., and Qiao, Y. (2023). Vision Transformer Adapter for Dense Predictions. *ArXiv:2205.08534* [cs].
- Choi, W.S., Olson, D.R., Davis, D., Zhang, M., Racson, A., Bingham, B., McCarrin, M., Vogt, C., and Herman, J. (2021). Physics-based modelling and simulation of multibeam echosounder perception for autonomous underwater manipulation. *Frontiers in Robotics and AI*, 8. DOI: 10.3389/frobt.2021.706646. URL <https://www.frontiersin.org/articles/10.3389/frobt.2021.706646>.
- Einsidler, D., Dhanak, M., and Beaujean, P.P. (2018). A deep learning approach to target recognition in side-scan sonar imagery. In: *OCEANS 2018 MTS/IEEE Charleston*, pp. 1–4. DOI: 10.1109/OCEANS.2018.8604879.
- Gonzalez, A.W., O’Keefe, P., and Williams, M. (2009). The UNESCO convention on the protection of the underwater cultural heritage: a future for our past? *Conservation and management of archaeological sites*, 11(1): 54–69.
- Kim, T., Kim, K., Lee, J., Cha, D., Lee, J., and Kim, D. (2022). Revisiting Image Pyramid Structure for High Resolution Salient Object Detection. *ArXiv:2209.09475* [cs].
- Lee, S., Park, B., and Kim, A. (2018). Deep learning from shallow dives: Sonar image generation and training for underwater object detection. *ArXiv:1810.07990* [cs].
- Lin, T., Hinduja, A., Qadri, M., and Kaess, M. (2023). Conditional gans for sonar image filtering with applications to underwater occupancy mapping. *IEEE*. DOI: 10.1109/icra48891.2023.10160646. URL <https://doi.org/10.1109>
- Liu, D., Wang, Y., Ji, Y., Tsuchiya, H., Yamashita, A., and Asama, H. (2021). CycleGAN-based realistic image dataset generation for forward-looking sonar. *Advanced Robotics*, 35(3-4): 242–254. DOI: 10.1080/01691864.2021.1873845. URL <https://doi.org/10.1080/01691864.2021.1873845>.
- MacLennan, D. (1986). Time varied gain functions for pulsed sonars. *Journal of Sound and Vibration*, 110(3): 511–522.
- Mittal, A., Soundararajan, R., and Bovik, A.C. (2013). Making a completely blind image quality analyzer. *IEEE Signal Processing Letters*, 20(3): 209–212. DOI: 10.1109/LSP.2012.2227726.
- Ochal, M., Vazquez, J., Petillot, Y., and Wang, S. (2020a). A comparison of few-shot learning methods for underwater optical and sonar image classification. In: *Global Oceans 2020: Singapore–US Gulf Coast*, IEEE, pp. 1–10.
- Ronneberger, O., Fischer, P., and Brox, T. (2015). U-net: Convolutional networks for biomedical image segmentation. In: *Medical Image Computing and Computer-Assisted Intervention–MICCAI 2015: 18th International Conference, Munich, Germany, October 5–9, 2015, Proceedings Part III*, 18. Springer, pp. 234–241.
- Santos, M.M.D., De Giacomo, G.G., Drews-Jr, P.L.J., and Botelho, S.S.C. (2022). Cross-view and cross-domain underwater localization based on optical aerial and acoustic underwater images. *IEEE Robotics and Automation Letters*, 7(2): 4969–4974. DOI: 10.1109/LRA.2022.3154482.
- Sechidis, K., Tsoumakas, G., and Vlahavas, I. (2011). On the stratification of multi-label data. In: *Machine Learning and Knowledge Discovery in Databases*, Berlin Heidelberg: Springer Berlin Heidelberg, pp. 145–158. ISBN: 978-3-642-23808-6.
- Sethuraman, A., and Skinner, K.A. (2022). Towards sim2real for shipwreck detection in side scan sonar imagery. In: *3rd Workshop on Closing the Reality Gap in Sim2Real Transfer for Robotics*.
- Sethuraman, A.V., and Skinner, K.A. (2023). Stars: Zero-shot sim-to-real transfer for segmentation of shipwrecks in sonar imagery. In: *34th British Machine Vision Conference 2023 BMVC 2023, Aberdeen, UK, November 20-24*
- Singh, D., & Valdenegro-Toro, M. (2021). The marine debris dataset for forward-looking sonar semantic segmentation. In: *2021 IEEE/CVF International Conference on Computer Vision Workshops (ICCVW)*.
- Sung, M., Kim, J., Kim, J., & Yu, S.C. (2019). Realistic sonar image simulation using generative adversarial network. *IFAC-PapersOnLine*, 52(21), 291–296.
- Thunder Bay National Marine Sanctuary (Accessed online: 2024). URL: <https://thunderbay.noaa.gov/>.
- Wang, J., Sun, K., Cheng, T., Jiang, B., Deng, C., Zhao, Y., Liu, D., Mu, Y., Tan, M., Wang, X., Liu, W., & Xiao, B. (2020). Deep High-Resolution Representation Learning for Visual Recognition. *arXiv:1908.07919* [cs].
- Xie, K., Yang, J., & Qiu, K. (2022). A dataset with multibeam forward-looking sonar for underwater object detection. *Scientific Data*, 9(1).
- Yang, D., Cheng, C., Wang, C., Pan, G., & Zhang, F. (2022). Side-scan sonar image segmentation based on multi-channel cnn for auv navigation. *Frontiers in Neurorobotics*, 16.
- Yang, D., Wang, C., Cheng, C., Pan, G., & Zhang, F. (2022). Semantic segmentation of side-scan sonar images with few samples. *Electronics*, 11(19).